Effect of Space Discretization on Phase Diagrams in Ionic Systems: A Field-Theoretic Approach

A. Ciach[1] and G. Stell[2]

[1]*Institute of Physical Chemistry, Polish Academy of Sciences 01-224 Warszawa, Poland*
[2]*Department of Chemistry, State University of New York, Stony Brook, New York 11794-3400, USA*

(Received 4 March 2003; published 4 August 2003)

Using Landau-Ginzburg-Wilson field-theoretic methods we determine for what kind of space discretization the transition between charge-disordered and charge-ordered phases in the restricted primitive model is fluctuation-induced first order. We identify this transition with ionic-crystal formation. We predict four types of generic phase diagrams in ionic systems for various kinds of space discretization for low and intermediate densities of ions. Our results also shed light on the simulation results obtained for an off-lattice ionic system over a wide range of densities, including the fcc crystal.

DOI: 10.1103/PhysRevLett.91.060601 PACS numbers: 05.70.Jk, 61.20.Qg, 64.60.–i, 82.45.–h

Recent theoretical and simulation results for ionic systems [1–5] seem to contradict the fundamental tenet of the theory of critical phenomena—the irrelevance of the short-length-scale properties of the system (in particular the space discretization) for the universal features of the phase diagrams [6]. Thanks to this fundamental property lattice models have been extensively used in calculations and simulations. Experimental phase diagrams in ionic solutions or molten salts [7] are correctly reproduced by the restricted primitive model (RPM) in which classical ions are modeled by charged hard spheres of equal charge e and diameter σ, interacting via Coulomb forces [8]. However, the phase diagrams of the lattice version of the RPM change character completely when the space discretization $n = \sigma/a$, (a is the lattice constant and $n \geq 1$) is varied from $n = 1$ to $n = 3$, i.e., for fixed σ the number of lattice sites per unit volume increases (for $n \rightarrow \infty$ the lattice sites become dense in R^3) [1–4]. For $n = 1$ order-disorder transition between a diluted uniform and a dense charge-ordered phase (with two oppositely charged sublattices) occurs. The transition is first order at low temperatures and changes into a line of continuous transitions (λ line) at the tricritical point (tcp) [1–4]. For $n = 2$ only a first-order order-disorder transition was found in simulations [2]. For $n \geq 3$, simulations show separation into uniform, ion-poor and ion-rich phases, terminated at the critical point, with no sign of the λ line and the tcp, as in the continuum RPM [2]. In the continuum RPM the critical point belongs to the Ising universality class [4,7–10], whose all members studied so far are characterized by phase diagrams having the same local properties in continuum and on different lattices. Very strong dependence of the phase diagrams on space discretization in the systems discussed here reveals a more complex nature of phase transitions and critical phenomena in ionic systems, and our work is aimed at elucidating the origin of this complexity. In addition to the fundamental importance of understanding this, there is a very practical side as well. Discretization is often used as a way of simplifying calculations and simulations, but it can only be so employed when its effects are well understood.

In this Letter we use Landau-Ginzburg-Wilson field-theoretic methods [6] to predict the change of character in the phase separation that occurs as one changes space discretization, as well as to illuminate closely related issues that are encountered at higher volume fractions, involving order-disorder transition between two fcc solid phases that has been discovered recently in simulations of the RPM [11]. A question that we shall address here is whether the order-disorder transition in the fcc solid has the same origin as the transition in the lattice models described above.

One can consider several extended-core models for increasing n: I—only the nearest-neighbor (nn) occupancy excluded, $n = \sqrt{2}$; II—second nn exclusion in addition, $n = \sqrt{3}$; and III—the third nn exclusion as well, $n = 2$. The simulations in Ref. [2] are for $n \geq 2$ only. One might expect model I to be closer in behavior to the continuum model, because each ion can have 12 neighbors at the distance of the closest approach, a_{nn}, while for $n = 2$ there are only six such neighbors, as on the simple cubic (sc) lattice. Moreover, in model I the uncharged reference system undergoes a transition to a phase in which only one sublattice (with the fcc structure) is occupied, which means one can hope to study in this model both its disordered "fluid" and its solid phases. We shall pay particular attention to model I in this Letter.

The Hamiltonian of the RPM model on the sc lattice with arbitrary n has the form

$$H = \frac{E_0}{2} \sum_{\mathbf{x},\mathbf{x}'} V_c(|\mathbf{x} - \mathbf{x}'|) g(|\mathbf{x} - \mathbf{x}'|) \hat{s}(\mathbf{x}) \hat{s}(\mathbf{x}') - \mu \sum_{\mathbf{x}} \hat{s}^2(\mathbf{x}), \tag{1}$$

where $\hat{s} = +1, -1, 0$ represents the anion, the cation, and the solvent, respectively. The lattice sites are $\mathbf{x} = x_i \mathbf{e}^i$, where $\mathbf{e}^i$ are the unit lattice vectors, x_i are integer numbers, $i = 1, 2, 3$, summation convention is used, and the distance is measured in a units. $\mu = (\mu_+ + \mu_-)/2 - \mu_0$

is the chemical potential. The energy unit is $E_0 = e^2 a_{nn}^2/(D v_0)$, where D is the dielectric constant of the solvent and v_0 is the volume per lattice site. The corresponding dimensionless temperature is $T^E = 1/\beta^E = kT/E_0$. The $V_c(|\mathbf{x}-\mathbf{x}'|)$ is the dimensionless Coulombic potential; $g(|\Delta\mathbf{x}|) = 0$ for forbidden pairs of sites and $g(|\Delta\mathbf{x}|) = 1$ otherwise. Different discretizations correspond to $g(|\Delta\mathbf{x}|) = 0$ for different values of $|\Delta\mathbf{x}|$. For $n = 1$ simultaneous occupancy of the lattice sites is excluded, and $g = 0$ only when $|\Delta\mathbf{x}| = 0$; for model I $g = 0$, also for $|\Delta\mathbf{x}| = 1$, etc.

On the mean field (MF) level that we shall consider here the grand potential Ω is approximated by [4]

$$\Omega[\phi, \rho] = F_{sr}[\phi, \rho] + U[\phi] - \mu \sum_{\mathbf{x}} \rho(\mathbf{x}), \qquad (2)$$

where $\rho = \langle \hat{s}^2 \rangle$, $\phi = \langle \hat{s} \rangle$ are the number and charge densities, respectively. $F_{sr}[\phi, \rho] = \sum_{\mathbf{x}} f_{sr}$ is the free energy of the uncharged reference system, containing the ideal-gas contribution and terms associated with the exclusion of occupancy of the forbidden pairs of sites. The internal energy $U[\phi]$ is approximated by

$$U = \frac{E_0}{2} \sum_{\mathbf{x},\mathbf{x}'} \phi(\mathbf{x}) V_c(|\mathbf{x}-\mathbf{x}'|) g(|\mathbf{x}-\mathbf{x}'|) \phi(\mathbf{x}'). \qquad (3)$$

The boundary of stability of Ω with respect to charge fluctuations $\tilde{\phi}(\mathbf{k})$ is given by $\tilde{C}^0_{\phi\phi}(\mathbf{k}_b) = 0$, where

$$\tilde{C}^0_{\phi\phi}(\mathbf{k}) \equiv \frac{\delta^2 \beta\Omega}{\delta\tilde{\phi}(\mathbf{k}) \delta\tilde{\phi}(-\mathbf{k})} = \frac{1}{\rho_0} + \beta^E \tilde{V}(\mathbf{k}), \qquad (4)$$

$\tilde{V}(\mathbf{k})$ (defined for $-\pi \le k_i \le \pi$) is the Fourier transform of $V_c(|\mathbf{x}-\mathbf{x}'|) g(|\mathbf{x}-\mathbf{x}'|)$, and at $\mathbf{k} = \mathbf{k}_b$ the $\tilde{V}(\mathbf{k})$ assumes a minimum. The first term in Eq. (4) results from the ideal-gas part in F_{sr}. The line of instability

$$T^E = S_\lambda \rho_0, \qquad S_\lambda = -\tilde{V}(\mathbf{k}_b) > 0 \qquad (5)$$

separates the uniform phase with $\phi = 0, \rho = \rho_0$ from the charge-ordered phase, where $\phi(\mathbf{x}) = \Phi \cos(\mathbf{k}_b \cdot \mathbf{x})$ for $T^E \to S_\lambda \rho_0$ from below; Φ corresponds to the minimum of Ω and is given by

$$\frac{\mathcal{A}_4}{4!} \Phi^2 = \frac{\beta^E}{2} (S_\lambda - T^E/\rho_0),$$
$$\mathcal{A}_4 = \frac{1}{\rho_0^3} \left[2 - \frac{3}{\rho_0 \tilde{C}^0_{\rho\rho}(0)} \right], \qquad (6)$$

where $\tilde{C}^0_{\rho\rho}(\mathbf{k})$ is defined by an expression analogous to (4). At the tcp, $\mathcal{A}_4 = 0$ and $T^E/\rho_0 = S_\lambda$. Different discretizations are associated with different forms of g, and in turn with different $\tilde{V}(\mathbf{k})$ and $\mathbf{k}_b$. Hence, the slopes of the MF line of instability (5) for different discretizations are different; for example, in the standard reduced units ($S^* = T^*/\rho^*$, $T^* = kTDa_{nn}/e^2$, and $\rho^* = \rho v$, where v is the volume per ion) $S^*_\lambda \approx 1.62$ and $S^*_\lambda \approx 3.2$ for $n = \sqrt{2}$ and $n = 2$, respectively.

The actual instability corresponds to singularity of $\langle \tilde{\phi}(\mathbf{k}_b) \tilde{\phi}(-\mathbf{k}_b) \rangle$, with the Boltzmann factor $\exp(-\beta\Omega)$. Beyond the MF $\langle \tilde{\phi}(\mathbf{k}) \tilde{\phi}(-\mathbf{k}) \rangle$ contains, in addition to $\tilde{C}^{0-1}_{\phi\phi}(\mathbf{k})$, the contribution $\sum_n a_n \mathcal{G}^n$, where $\mathcal{G} = \int_{\mathbf{k}} \tilde{C}^{0-1}_{\phi\phi}(\mathbf{k})$, and less relevant terms [6,12]. Because $\tilde{C}^{0-1}_{\phi\phi}(\mathbf{k}) \to \infty$ for $\mathbf{k} \to \mathbf{k}_b$ when $T^E/\rho = S_\lambda$, the value of $\mathcal{G}$ depends on the position and the region of $\mathbf{k}_b$ in $\mathbf{k}$ space. In continuum $\mathbf{k}_b$ form a surface of finite area [4,13] and $\mathcal{G}$ diverges when $T^E/\rho = S_\lambda$. The MF approximation breaks down when $\mathcal{G}$ diverges, and the fluctuation-induced first-order phase transition can be expected [12,14]. On the sc lattice $\mathbf{k}_b = \pi(\pm 1, \pm 1, \pm 1)$, i.e., $\mathbf{k}_b$ form the vertices of the cubic domain in $\mathbf{k}$ space [4,13]. For $n = 2$ we find, using the appropriate choice for $g(|\mathbf{x}-\mathbf{x}'|)$ that $\mathbf{k}_b$ are isolated vectors located inside the domain. $\mathcal{G}$ is finite in both models. A more detailed analysis of these two models [15] is based on a transformation of the functional of the single critical field $\tilde{\phi}(\mathbf{k})$, with several critical vectors $\mathbf{k}^i_b \neq \mathbf{0}$, to a functional of several fields $\tilde{\psi}_i(\mathbf{q})$, with $\mathbf{q} = \mathbf{0}$ for the critical modes [16,17]. On the sc lattice the functional can be reduced to the standard "φ^4" Landau functional, and the transition remains continuous. For $n = 2$ the functional reduces to the functional similar to the one obtained for type II antiferromagnets [18], and there is no stable fixed point of the renormalization-group flow equations [15]; therefore the transition should be first order.

The instability of the disordered phase is induced either by $\phi(\mathbf{x}) \propto \cos(\mathbf{k}_b \cdot \mathbf{x})$ or by the whole spectrum of the charge fluctuations, associated with the shift of the number density of ions [4]. The latter instability can be found after the charge fluctuations are integrated out [4]. Hence, the spinodal line has two branches; the low-density part of the spinodal is associated with a phase separation into two uniform (charge-disordered) phases [4,9] and depends on the presence and the kind of the underlying lattice rather weakly [19]. The high-density branch of the spinodal has different slopes S^*_λ on different lattices already in the MF. Moreover, the larger the volume of dominant fluctuations, $\mathbf{k} \approx \mathbf{k}_b$, in $\mathbf{k}$ space, the larger the shift of the spinodal line compared to the MF prediction. For small slopes of the high-density branch of the spinodal the phase diagrams should have the form shown in Figs. 1(b) and 1(d). The diagrams obtained for $n = 1, 2$ and in continuum are shown in Figs. 1(a), 1(c), and 1(d), respectively. They all agree with simulations [2]. The diagram shown in Fig. 1(b) has been obtained in simulations [5] for the RPM supplemented with dispersionlike forces.

Let us analyze model I for the whole range of densities. For the reference system in (2) we assume the form of F_{sr} derived in Ref. [20]. The reference system undergoes a transition to a nonuniform state at $\rho_0 \approx 0.18$ [20]. In the nonuniform phase two sublattices are formed, with different density at each sublattice. For $\rho_0 > 0.3$ only the lattice points $\mathbf{x} = x_i \mathbf{e}^i$ whose coordinates are $(i + j, i + k, j + k)$, where i, j, k are integer, are not empty. The

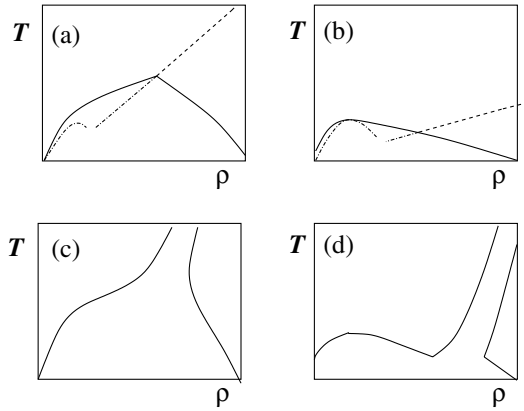

FIG. 1. Generic types of phase diagrams in the RPM for different space discretizations for low and intermediate concentrations of ions ρ. Solid and dashed lines are first-order and continuous transitions, respectively, and the dashed-dotted lines are the spinodals associated with the gas-liquid and order-disorder transitions. The dashed lines are given by Eq. (5) in MF, and, as discussed below, their slopes are decreased by fluctuations [15]. The low-density parts of the spinodals are given by the formal expression derived in Ref. [4]. In (c) and (d) the spinodals should be similar to those shown in (a) and (b), respectively, but their precise location (beyond MF) has not been determined yet. Solid lines are schematic. The low-density phases are charge disordered, and the high-density phases are charge ordered. The charge-disordered phase undergoes a transition into ion-diluted and ion-dense phases in the cases (b) and (d). There are two variants in case (b), depending on the shape of the high-density branch of the spinodal line; namely, the line of continuous transitions can meet the line of first-order transitions at the critical endpoint, or at the tcp.

occupied sublattice has the fcc structure, with the linear size of the unit cell $a_{\mathrm{fcc}} = 2a$. Simple algebra described in [15] shows that the instability of the charge-disordered phase is associated with the bifurcation vectors $\mathbf{k}_b = (0, \pm\pi, q)$ (and vectors obtained by permutations of the above coordinates). In real space the critical fluctuations have the form

$$\phi(i + j, i + k, j + k) = (-1)^{i+k}\Phi\{\mathrm{Re}(w)\cos[q(j + k)] + \mathrm{Im}(w)\sin[q(j + k)]\}, \tag{7}$$

where $ww^* = 1$. The structure found in simulations in the continuum RPM at close packing in Ref. [11] is given by Eq. (7) with $q = \pi/2$ and $w = (1 + i)/\sqrt{2}$. $\mathcal{G}$ diverges at the MF line of instability [15], and the fluctuation-induced first-order phase transition can be expected, in agreement with simulations [21].

In the low-density, fluid regime ($\rho_0 < 0.18$), the tcp can be obtained numerically in the MF from the condition $\mathcal{A}_4 = 0$, Eq. (6) and from the form of $\tilde{C}^0_{\rho\rho}$ given in Ref. [20]. The result is

$$\rho_{tc} = 0.0608, \quad \text{and} \quad \rho^*_{tc} \approx 0.12. \tag{8}$$

ρ^*_{tc} is quite close to $\rho^*_{tc} \approx 0.1$, the value obtained within analogous treatment [13] of the continuum RPM using a Percus-Yevick reference-system approximation. In the RPM reduced units $S^*_\lambda \approx 1.62$, i.e., very close to $S^*_\lambda \approx 1.61$ found in the continuum RPM. Moreover, the coordinates k^i_b of the bifurcation vectors satisfy the equation [15]

$$\sum_i^3 \cos k^i_b = \mathrm{const} \approx 1.29, \tag{9}$$

i.e., form a surface of finite area and $\mathcal{G}$ diverges, as in the continuum model. Such fluctuations should lead to a very large shift of S^*_λ, and to the fluctuation-induced first-order phase transition, hence—to the phase diagram shown in Fig. 1(d).

Let us focus on $T \to 0$. The charge-ordered fcc structure, shown in Fig. 2(b), is stable for $\rho_0 = 1/2$. At $\rho_0 = 1/4$ only the sites with integer coordinates $(i + j - k, i - j + k, -i + j + k)$ are occupied. These sites form a bcc sublattice, with the lattice constant of the unit cell $a_{\mathrm{bcc}} = 2a$. This bcc sublattice splits again into two sublattices, one positively, the other one negatively charged. At very low T one should expect stability of the bcc charge-ordered solid, whose electrostatic energy is low, then bcc—gas (vacuum) phase coexistence at lower densities, and bcc—fcc phase coexistence at higher densities. It is instructive to consider the order-disorder transition on the bcc sublattice. Using the appropriate form of $\tilde{V}$ and the method described above, we find that in MF $S^*_\lambda = 3.98$. At T higher than the transition temperature, the bcc charge-disordered phase is more stable than the charge-ordered phase. However, the stability of the charge-disordered phases is entirely determined by the uncharged reference system. In the latter the stability of the bcc solid

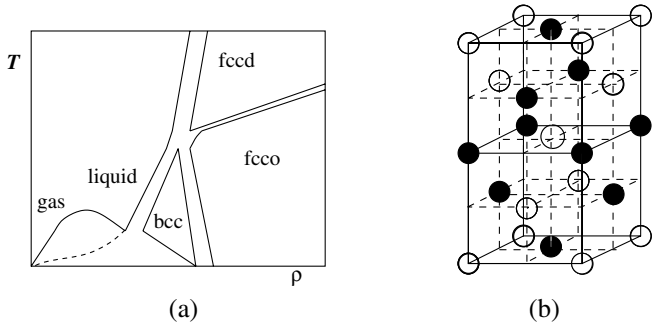

FIG. 2. (a) Schematic phase diagram for model I. The dotted line is the line of the metastable transition between the charge-disordered and charge-ordered phases. The whole phase diagram contains the gas-liquid and the order-disorder transitions [Fig. 1(d)], the formation of the fcc solid, determined by the uncharged reference system, and the order-disorder transition in the fcc solid. We assumed that the charge-ordered phase coexisting with the liquid phase has the bcc structure. (b) Charge-ordered fcc structure [denoted by "fcco" in (a)], given by Eq. (7) with $q = \pi/2$ and $w = (1 + i)/\sqrt{2}$.

(bcc sublattice occupied) is not expected [20]. We can conclude that at temperatures higher than the charge-ordered–charge-disordered transition line on the bcc sublattice, the fluid phase is stable in model I. We identify the fluid—charge-ordered bcc solid transition with the fluctuation-induced first-order order-disorder transition discussed before. Our results for model I are summarized in Fig. 2(a). Note the close similarity to the diagram obtained in simulations for the continuum RPM [11] for the whole range of densities. The $n = 1$ model can be transformed continuously into model I, if a repulsion between nearest neighbors of a strength $J > 0$ is present, and the Hamiltonian on the sc lattice has the form

$$H_J = \frac{1}{2}\sum_{\mathbf{x}}\sum_{\mathbf{x}'\neq\mathbf{x}} V_c(|\mathbf{x}-\mathbf{x}'|)\hat{s}(\mathbf{x})\hat{s}(\mathbf{x}') + \frac{J}{2}\sum_{\mathbf{x}}\sum_{\mathbf{x}'=\mathbf{x}\pm\mathbf{e}^i}\hat{s}^2(\mathbf{x})\hat{s}^2(\mathbf{x}') - \mu\sum_{\mathbf{x}}\hat{s}^2(\mathbf{x}). \quad (10)$$

The probability that the nn lattice sites are occupied is $\propto e^{-\beta J}$, hence it vanishes for $J = \infty$, and we obtain model I. For the model given by (10) we include the nn repulsion in the reference system, for which the Bethe approximation [22] is assumed. For U in (3) we assume the form of g consistent with the above approximation, namely, $g(|\mathbf{x}-\mathbf{x}'|) = 0$ if $\mathbf{x} = \mathbf{x}'$, $g(|\mathbf{x}-\mathbf{x}'|) = \exp(-\beta J) \equiv 1 - p$ if $\mathbf{x} - \mathbf{x}' = \pm\mathbf{e}_i$, and $g(|\mathbf{x}-\mathbf{x}'|) = 1$ otherwise. Using the method described above we find that $\mathbf{k}_b = (\pm\pi, \pm\pi, \pm\pi)$, as for $n = 1$, as long as $p \leq p_0$, with $p_0 \approx 0.0807$ [15], whereas for $p \geq p_0$, $\sum_i^3 \cos k_b^i = 3(1 - 2\sqrt{p_0/p})$, i.e., $\mathbf{k}_b$ form a surface, as for model I. For $p \approx p_0$ the crossover between continuous and first-order order-disorder transition occurs, due to a change of the fluctuation volume in $\mathbf{k}$ space. In the MF both ρ_{tc} and S_λ (for $p \leq p_0$) decrease for increasing p. Whether the critical point becomes stable for p smaller or larger than p_0 depends on the exact value (beyond MF) of S_λ^*. Further studies are required to verify whether the sequence of phase diagrams in Fig. 1 is $(a) \rightarrow (b) \rightarrow (d)$, or $(a) \rightarrow (c) \rightarrow (d)$, as p increases.

The phase behavior in the RPM is determined by the charge fluctuations—the dominant ones, $\tilde{\phi}(\mathbf{k}_b)$, leading to the order-disorder transition, and by the whole spectrum, leading to the gas-liquid separation [4]. The order [compare Figs. 1(a) and 1(b) with Figs. 1(c) and 1(d)] and the location [compare Figs. 1(a) and 1(c) with Figs. 1(b) and 1(d)] of the order-disorder transition are determined by the position and extension of the region occupied by $\mathbf{k}_b$ in $\mathbf{k}$ space. As we have shown, both the position and the extension of $\mathbf{k}_b$ depend crucially on space discretization. It is the order-disorder transition, which depends on discretization, and the location of this transition determines whether the critical point is stable or metastable.

We thank A. Z. Panagiotopoulos for helpful conversations and for sending us a draft of Ref. [5]. The support of the Division of Chemical Sciences, Office of the Basic Energy Sciences, Office of Energy Research, U.S. Department of Energy is gratefully acknowledged; this work was also supported by the KBN Grant No. 4T09A06622 (A. C.).

[1] R. Dickman and G. Stell, in *Proceedings of the Conference Treatment of Electrostatic Interactions in Computer Simulations of Condensed Media, Santa Fe, 1999*, edited by G. Hummer and L. R. Pratt (AIP, New York, 1999); see also G. Stell, in *New Approaches to Problems in Liquid-State Theory*, edited by C. Caccamo, J.-P. Hansen, and G. Stell (Kluwer Academic Publishers, Dordrecht, 1999), p. 71.
[2] A. Z. Panagiotopoulos and S. K. Kumar, Phys. Rev. Lett. **83**, 2981 (1999).
[3] A. Brognara, A. Parola, and L. Reatto, Phys. Rev. E **65**, 066113 (2002).
[4] A. Ciach and G. Stell, J. Mol. Liq. **87**, 253 (2000); Physica (Amsterdam) **306A**, 220 (2002); J. Chem. Phys. **114**, 382 (2001).
[5] A. Diehl and A. Z. Panagiotopulos, J. Chem. Phys. **118**, 4993 (2003).
[6] D. J. Amit, *Field Theory, the Renormalization Group and Critical Phenomena* (McGraw Hill, New York, 1978).
[7] M. Kleemeier, S. Wiegand, W. Schröer, and H. Weingärtner, J. Chem. Phys. **110**, 3085 (1999).
[8] B. Hafskjold and G. Stell, in *The Liquid State of Matter. Fluids, Simple and Complex*, edited by E. N. Montroll and J. L. Lebowitz (North-Holland, Amsterdam, 1982), Sec. 6.4.
[9] G. Stell, Phys. Rev. A **45**, 7628 (1992); J. Stat. Phys. **78**, 197 (1995).
[10] E. Luijten, M. E. Fisher, and A. Z. Panagiotopoulos, J. Chem. Phys. **114**, 5468 (2001).
[11] F. Bresme, C. Vega, and J. L. F. Abascal, Phys. Rev. Lett. **85**, 3217 (2000).
[12] S. A. Brazovskii, Sov. Phys. JETP **41**, 85 (1975).
[13] A. Ciach and G. Stell, J. Chem. Phys. **114**, 3617 (2001).
[14] Y. Levin, C. J. Mundy, and K. A. Dawson, Phys. Rev. A **45**, 7309 (1992).
[15] A. Ciach and G. Stell (to be published).
[16] S. Krinsky and D. Mukamel, Phys. Rev. B **16**, 2313 (1977).
[17] Y. Levin and K. A. Dawson, Phys. Rev. A **42**, 1976 (1990).
[18] D. Mukamel and S. Krinsky, Phys. Rev. B **13**, 5078 (1976).
[19] V. Kobelev, A. B. Kolomeisky, and M. E. Fisher, J. Chem. Phys. **116**, 7589 (2002).
[20] B. Jancovici, Physica (Amsterdam) **31A**, 1017 (1965); D. S. Gaunt and M. E. Fisher, J. Chem. Phys. **43**, 2840 (1965).
[21] N. G. Almarza and E. Enciso, Phys. Rev. E **64**, 042501 (2001).
[22] T. L. Hill, *Statistical Mechanics. Principles and Selected Applications* (McGraw-Hill Book Company, New York, 1956).